Journal of Applied Polymer Science

Effects of titanate treatment on morphology and mechanical properties of graphene nanoplatelets/high density polyethylene nanocomposites

Pashupati Pokharel,[1] Hyunmin Bae,[1] Jung-Gyu Lim,[1] Kyoung Yong Lee,[2] Sunwoong Choi[1]

[1]Department of Polymer Science and Engineering, Hannam University, Daejeon 305-811, Republic of Korea

[2]Lotte Chemical 115, Gajeongbuk-ro, Yuseong-gu, Daejeon 305-726, Republic of Korea

Correspondence to: P. Pokharel (E-mail: ppokharel2008@gmail.com) and S.W. Choi (E-mail: swchoi@hnu.ac.kr)

ABSTRACT: The effect of graphene nanoplatelets (GNPs) and titanate coupling agent on morphology and mechanical properties of high density polyethylene (HDPE) nanocomposites was investigated. The titanate has a tendency to link chemically with the two dissimilar species GNPs and HDPE via proton coordination to generate a complete continuous phase for stress/strain transfer via the elimination of air voids and hydrophobicity. The interaction of titanate with GNPs and HDPE was effective to improve the dispersion of GNPs in HDPE composites. At constant weight (1 wt %) of titanate treatment for 2 and 5 wt % HDPE composites, we clearly observed a significantly high value of tensile strength and elongation at break than untreated composites. Particularly, composite containing 2 wt % GNPs in HDPE with titanate showed 66.5% improvement of the ultimate tensile strength and an enormously high value of elongation at break. The effect of GNPs dispersion and orientation in HDPE for the mechanical reinforcement was also evaluated based on the experimental modulus data to theoretical predictions made using the Halpin-Tsai model. © 2015 Wiley Periodicals, Inc. J. Appl. Polym. Sci. **2015**, *132*, 42073.

KEYWORDS: composites; mechanical properties; polyolefins; thermal properties

Received 27 October 2014; accepted 2 February 2015

DOI: 10.1002/app.42073

INTRODUCTION

Among the commodity plastics, polyolefins have a superior rank due to their use in a variety of applications like containers, toys, home appliances, engineering plastics, automotive parts, adhesives, medical applications, etc. High-density polyethylene (HDPE) possesses wide range of properties including good processability, nontoxicity, ease of recycling, biocompatibility, low cost, and good chemical resistance.[1–3] To meet the demands of new applications, it is required to improve the performance of HDPE in terms of properties such as stiffness and rigidity by forming composites.[4–6] Incorporation of the carbon nanofillers in the polymer matrix can produce light weight nanocomposites with better physical and mechanical properties even at a low filler concentration than the conventional composites. The composite of HDPE can fulfill the requirements for different applications such as cost and weight reduction, heat stability, dimensional stability, opacity, and processability.

In the nanocomposite, a completely different interfacial morphology is observed as compared with the bulk polymer[4,6] due to the higher number of interfacial contacts of nanofillers with the polymer chains. The excellent electrical, thermal, and mechanical properties of graphene have already enthralled the attention of researchers for the generation of polymer nanocomposites.[7–12] A single defect-free graphene layer possesses excellent gas impermeability, specific surface area of ~2600 m^2/g, Young's modulus of ~1.0 TPa, and thermal conductivity ~6000 W/m K.[13] Graphite is the parent material of graphene that is present in nature prolifically. Intercalation and exfoliation of graphite can generate graphene nanoplatelets (GNPs),[14] and that are very useful for the preparation of the polymer nanocomposites.[15] Uniform transfer of the superior properties of the nanofillers to the host polymer matrix leads to the full advantage of the nanofiller for the mechanical reinforcement.[16–18] The macroscopic properties of polymer nanocomposites[17,18] are directed by thermodynamic factors such as an interfacial compatibility of the polymer and the filler phases, polarity match between the filler surface and the polymer chains. Generally, dispersion techniques, time of mixing, and applied shear determine the nanoscale dispersion and distribution of the filler in the polymer matrix.[19–21] Most of the research works have been focused to achieve the full strength of the nanofillers by using different mixing techniques, modification of polymer backbone or filler surface, use of compatibilizer

and coupling agents, etc.[22–30] Pollanen *et al.*[22] prepared a masterbatch of carbon nanotube with maleic anhydride grafted polyethylene (PEgMA) as a polymeric compatibilizer and studied the morphological, thermal, mechanical, and tribological properties of HDPE. In their study, the unmodified and modified (hydroxyl or amine groups) CNTs showed similar effects on the properties of HDPE–PEgMA as an indication of noncovalent interactions between CNTs and matrix. Mittal *et al.*[10] showed significant changes in the microstructure of HDPE and chlorinated polyethylene (CPE) blends, as well as their composites with GO. In their composite, the surface of GO was surrounded with a hard phase due to enhanced nucleation action of the graphene platelets as well as ordering of CPE chains near the graphene surface.

For the preparation of HDPE nanocomposites, the lack of polar groups on the backbone of polyethylene[1–3] is a hurdle for the homogenous dispersion and exfoliation of nanofillers.[5] Incorporation of the coupling agent having polar and nonpolar groups can act as bridges between filler and host polymer and that can improve the dispersion of fillers in the polymer matrix.[23–30] Alkadasi *et al.*[30] treated the surface of fly ash with a titanate coupling agent and prepared a composite with polybutadiene rubber. The large improvement on the tensile strength and Young's modulus was observed in their study after the incorporation of titanate treated fly ash in rubber. The titanate coupling agents are proton (H^+) reactive via solvolysis (monoalkoxy) or coordination (neoalkoxy) without the need of water of condensation while the silane are hydroxyl (OH^-) reactive via a silanol-siloxane mechanism involving condensation of water.[31] Many nanofillers, particulates and fibers, which are used for reinforcing thermoplastics and thermosets do not have surface silane reactive hydroxyl groups. Almost all particulates and other species such as calcium carbonate, graphite, GNPs, boron, and aramid or other organic derived fibers have surface protons and that are generally more reactive with titanates than silanes.[23–28,31] Li *et al.*,[32] reported the covalently bonding of the titanate on the surface of graphene, and the electrical percolation threshold of the composite was achieved at 0.1 wt % loading in PU matrix. Leong *et al.*[33] showed the effect of the surface treatment of fillers by three different coupling agents (titanate, silane, and stearic acid) on the mechanical, thermal, and morphological properties of polypropylene (PP) composites. They observed the large improvement of elongation at break of calcium carbonate filled PP composite due to the plasticizing effect of the titanate coupling agent. In their study, the improved dispersion and orientation of the filler particles and the plasticizing effect of the titanate coupling agent facilitated the better impact properties of the titanate-treated talc-filled PP composites than without the treatment with coupling agent.

Even there are many advantages of the addition of titanate coupling agent[31] during the preparation of polymer composites; there are not any reports that show the effect of titanate on the functional properties of GNPs/HDPE composite till now. In this study, the titanate coupling agent was employed as a dispersing agent as well as a compatibilizer in order to improve the dispersion of GNPs in HDPE with strong adhesion. A solution mixing technique was employed for the preparation of GNPs based HDPE composite with titanate. The effect of GNPs along with titanate on the morphology, thermal, and mechanical properties of the GNPs/HDPE nanocomposites was studied.

EXPERIMENTAL

Materials

High density polyethylene (HDPE) powder with density (ρ) of 0.95 g/cm^3, melting temperature (T_m) of 130°C was supplied by Lotte Chemical, South Korea. Titanate coupling agent (LICA-12) was purchased from GS Seyoun Chemical Trading Company, South Korea and used as received. GNPs were prepared from natural graphite via intercalation and exfoliation with tetraalkylammoniumbromide.[14] Xylene, tetrahydrofuran (THF) and ethyl alcohol were purchased from Samchun Chemical, South Korea.

Preparation of GNPs/HDPE Thin Film

A solution dispersion method was employed for the preparation of HDPE composites having GNPs content of 2, 5, and 10 wt % with constant weight of titanate (1 wt %) treatment. Typically, for the preparation of 2 wt % GNPs/HDPE nanocomposite with titanate, solution of titanate coupling agent in isopropyl alcohol was prepared after dispersing 0.3 g titanate in 320 mL isopropyl alcohol. Then, GNPs (0.6 g) was added to the titanate solution and carried out ultrasonication for 3 h. On the other hand, HDPE powder (29.4 g) was completely dissolved in 1600 mL xylene at 90°C for 6 h. The stable GNPs/IPA suspension with titanate prepared by the aforementioned method was then quickly added into the xylene-HDPE solution and continuously stirred further 1 h. The mixture was flocculated using ethanol, and was then filtered, and dried in an oven for 3 days at 90°C. Same method was followed for the preparation of 5 and 10 wt % GNPs based HDPE composite with titanate. HDPE composites containing 2 and 5 wt % GNPs without titanate treatment was also prepared at the same conditions for the comparison. Finally, neat HDPE powder as well as titanate treated and untreated GNPs/HDPE composite powder were compression molded in a hot press for 7 min under 750 bar at a temperature of 190°C to form square sheets ($12 \times 12 \times 0.5$ mm^3) and used for characterization.

Characterization

A transmission electron microscope (TEM; JEOL 2100 microscope, Japan) at 200 kV was used to determine the morphological features as well as thickness of the GNPs. A sample for TEM measurement was prepared after 3 h sonication of GNPs dispersion in isopropyl alcohol (0.01 mg/mL) and the copper grid was dipped in the suspension and dried in the oven for 3 h at 60°C. A wide angle X-ray scattering (WAXS) of the GNPs and GNPs/HDPE nanocomposites was performed on Rigaku X-ray diffractometer using the Cu Ka radiation ($k = 1.54184$ nm). An image plate ~6 cm from the sample position was used to calculate the X-ray intensity. For the conversion of exact pixel-to-angle, silver behenate was used. Two-dimensional WAXS patterns were collected and converted into q and 2θ values using our computer software program. The nature of GNPs, especially the defect and order of graphitic layer, were determined by Raman scattering (633 nm, neon laser). Fourier Transforms Infrared (FTIR) spectra of the nanocomposites were recorded on FTIR spectrometer in ATR mode. The melting as well as crystallization

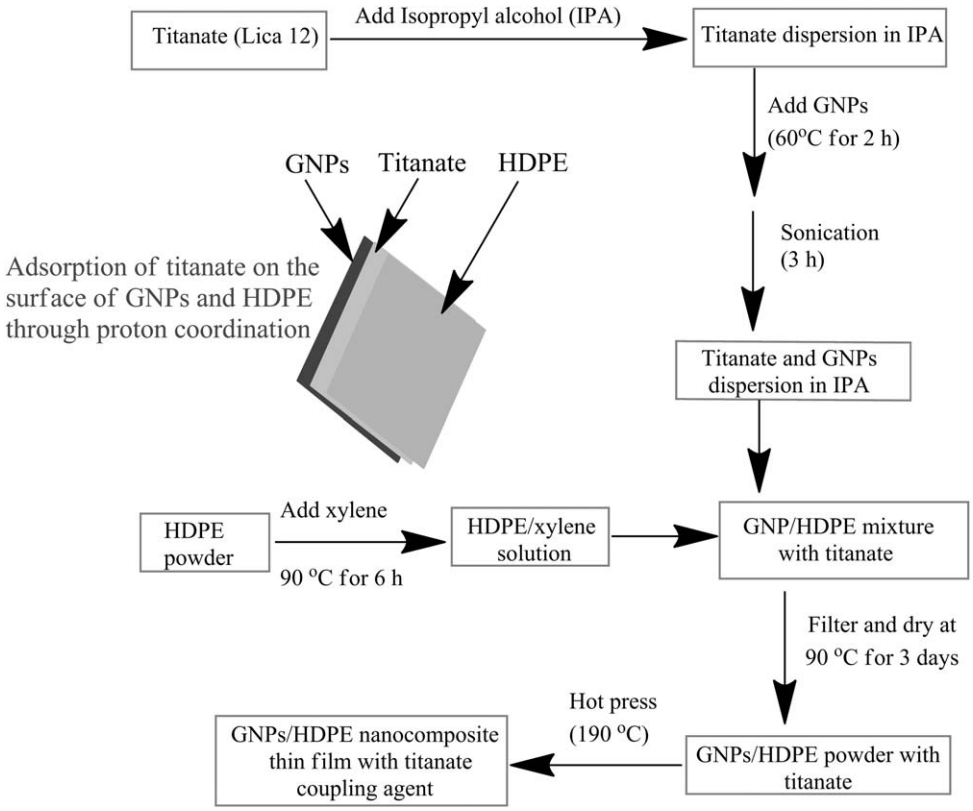

Figure 1. Schematic diagram for the fabrication process of the GNPs/HDPE composites with neoalkoxy titanate.

behaviors of GNPs/HDPE composites were determined using a TA 2910 differential scanning calorimeter (DSC), with a constant heating rate of 10°C/min and the same cooling rate from 25 to 200°C. The melting and crystallization temperatures, enthalpies of melting and crystallization as well as the percentage crystallinity of neat HDPE and composites were determined from the second heating-cooling cycle. Tensile tests were performed at room temperature on a universal testing machine (Shimadzu Corporation, Japan) with a cross head speed of 5 mm/min according to the ASTM D638-10, type IV specification. The average values of the three samples were used for plotting the ultimate tensile strength, Young's modulus, and elongation at break of neat HDPE and GNPs/HDPE composites. Fracture surfaces of neat HDPE and nanocomposites after tensile test were coated with gold and then observed in a scanning electron microscope (Mini-SEM SNE- 4500M). The cryogenically fracture surfaces of 2 and 5 wt % GNPs/HDPE composites with titanate were examined using a scanning electron microscopy (SEM, JSM-6700, JEOL, Japan).

RESULTS AND DISCUSSION

Figure 1 shows the fabrication process of the GNPs/HDPE composites with neoalkoxy titanate. The addition of titanate during the preparation of GNPs/HDPE composites can improve the interfacial adhesion between the fillers and matrix. The titanate coupling agent is thermally stable and can develop for high-temperature applications, above 200°C in the absence of water. They react via a coordination mechanism with free protons on the filler surface, generating no by-product or leaving group.[31] Almost all particulates contain free protons react with titanates and generate an organic monomolecular layer at the inorganic surface. Molecular bridges between the surface of GNPs and HDPE are formed by titanate coupling agents.[34] Titanate coupling agent not only improves filler dispersion and enhancing the properties and processing of the composites but also acts as plasticizers for facilitating higher filler loadings, and as catalysts for a number of reactions in the polymer matrix.[31] TEM image of the GNPs in Figure 2(a) shows the thin folded paper like graphene sheet on TEM grid.[14] The HR-TEM image of GNPs in Figure 2(b) shows numerous graphitic layers at the edge having thickness ~8 nm. Figure 3 shows (a) two-dimensional (2D) wide angle X-ray scattering (WAXS) of GNPs and (b) corresponding X-ray diffraction after data conversion into 2θ values, in which the characteristic diffraction peak of GNPs (002) was observed at 2θ value 26.3°. Raman spectroscopy has been widely used for the characterization of carbon nanomaterials and can explain in terms of D/G ratio.[14,15] The Raman spectrum of GNPs in Figure 3 (c) shows the D-band and G-band at 1367 and 1613 cm^{-1}, respectively as well as the calculated D/G ratio 0.78. The interaction of natural graphite with lithium metal and subsequent microwave exfoliation generated defects on the surface of graphene sheets as a result the disorder in the sp^2 carbon lattice of GNPs was observed.[14]

In our study, the objective of the addition of titanate during the preparation of HDPE composite is to improve the adhesion between the GNPs and HDPE through proton coordination.[34] After the incorporation of 1 wt % titanate for the surface treatment of GNPs, the unbounded fraction of titanate with GNPs

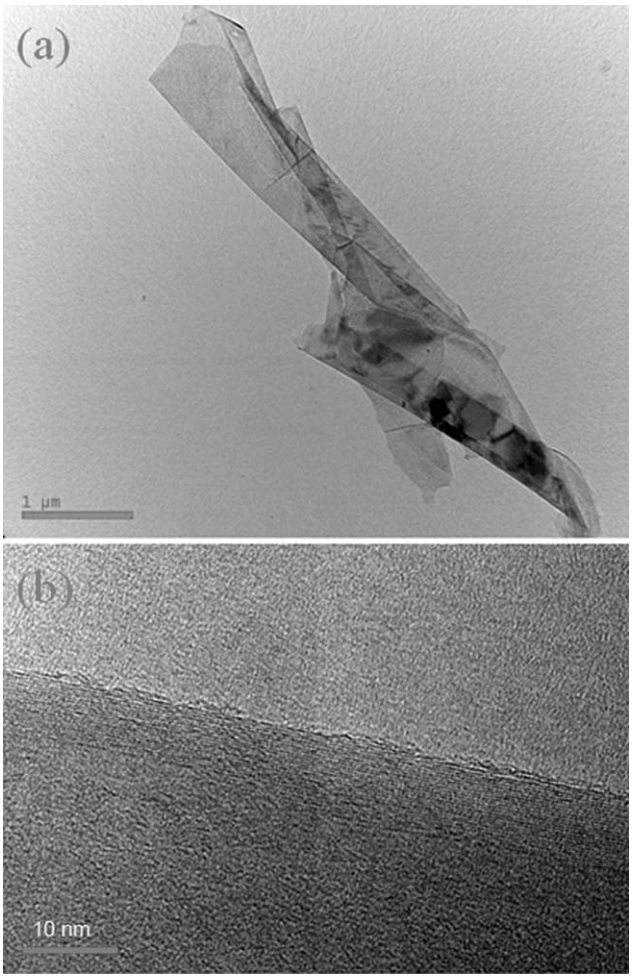

Figure 2. (a) TEM image of GNPs and (b) HR-TEM image of GNPs. Scale bar is 1 μm for (a) and 10 nm for (b).

and HDPE was removed at the filtration step of the flocculated composite in solvents. The photographs of (a) neat HDPE and (b) 2 wt % GNPs/HDPE with titanate are shown in Figure 4. The white color of HDPE film was completely changed into homogenously dark black color with the addition of 2 wt % GNPs. Figure 5 shows the FTIR spectra of titanate, neat HDPE, and 2 wt % GNPs/HDPE with titanate. It was difficult to show the clear differences between the HDPE and GNP/HDPE composite with titanate through IR measurement due to the overlapping of the some characteristic absorption peaks of titanate with HDPE[10] in composites. However, a close examination of IR spectra showed broadening the absorption band (V_a CH_2) of PE at 2914 cm^{-1} in composite. Furthermore, new absorption bands at 1646 and 1727 cm^{-1} were observed in composites similar to the titanate coupling agent. Such changes were possibly occurred due to the adsorption of titanate in HDPE composite through proton coordination.

The mechanical properties of the neat HDPE and GNPs/HDPE nanocomposites were examined by the tensile test measurements. Figure 6 shows the stress-strain plot of (a) neat HDPE, (b) 2 wt %, and (d) 5 wt % GNPs/HDPE composites without titanate. It was clear that 2 wt % loading of GNPs in HDPE significantly improved the ultimate tensile strength and elongation at beak of composite. Further increasing the concentration of GNPs increased Young's modulus, but decreased the ultimate tensile strength and elongation at beak of the composite. The stress–strain plot of (c) 2 wt %, (e) 5 wt %, and (f) 10 wt % GNPs/HDPE composites with titanate in Figure 6 confirmed the better improvement of the tensile strength, elongation at break, and modulus of the composites with titanate than without titanate. The extracted data of ultimate tensile strength, Young's modulus, and elongation at break of GNPs/HDPE composites with and without titanate are shown in Figure 7 and Table I. The titanate treated GNPs/HDPE composites showed that the treatment had the great effect on the tensile strength and elongation at break as compared to untreated GNPs. Furthermore, 2 wt % GNP/HDPE with titanate showed strong strain hardening effect, possibly because the stretched HDPE with GNPs and titanate at certain concentration intensified the ability to resist further deformation. The ultimate tensile strength of the 2 wt % GNP/HDPE composites with titanate treated and untreated showed an increase of 66.5% and 34.04%, respectively as compared with the neat HDPE (18.8 MPa). However, the tensile modulus of both titanate treated and untreated 2 wt % GNPs/HDPE composite showed slightly improvement in modulus. Probably, a plasticizing effect of the titanate[33] was responsible for small increase of modulus with the incorporation of 2 wt % GNPs/HDPE composite with titanate. On the other hand, relatively poor interaction of GNPs with HDPE without titanate treatment was accountable for the slightly improvement of the modulus of 2 wt % GNP/HDPE composite. The plasticizing effect of titanate was insignificant at higher concentration of GNPs as a result large improvement of modulus was observed for 5 wt % GNPs/HDPE composites [Figure 7(b)]. The increase in the tensile strength and the deformability of the HDPE composites showed positive coupling effects of the titanate on both HDPE and GNPs. We believe that our method of the titanate treatment on the surface of GNPs and HDPE was useful to obtain homogeneity and adequate coupling with correct dosage between the fillers and matrix, because the excess titanate (unbounded form) was removed during the filtration of the flocculated composite mixture. The elongation at break for 2 wt % composite with the coupling agent increased enormously and still nearly equal to neat HDPE even 5 wt % composite as shown in Figure 7(c). This drastic improvement in deformability further suggests that the coupling between the filler and matrix was not strong enough because the fillers failed to hinder plastic deformation of the polymer matrix.[33] Furthermore, the large improvement on the tensile strength and the toughness of the composites could be attributed to the improved dispersion and orientation of the GNPs and the plasticizing effect of the titanate coupling agent. There are not any reports in the literature of GNPs/HDPE composites having such a high elongation at break along with the large improvement of the ultimate tensile strength.[4,20,35] Generally, the coupling of the titanate to the inorganic/organic substrate in 2 nm atomic monolayer allows for the elimination of air voids, hydrophobicity, and a complete continuous phase is formed for stress/strain transfer.[34] The strong interfacial bond between filler and matrix not only

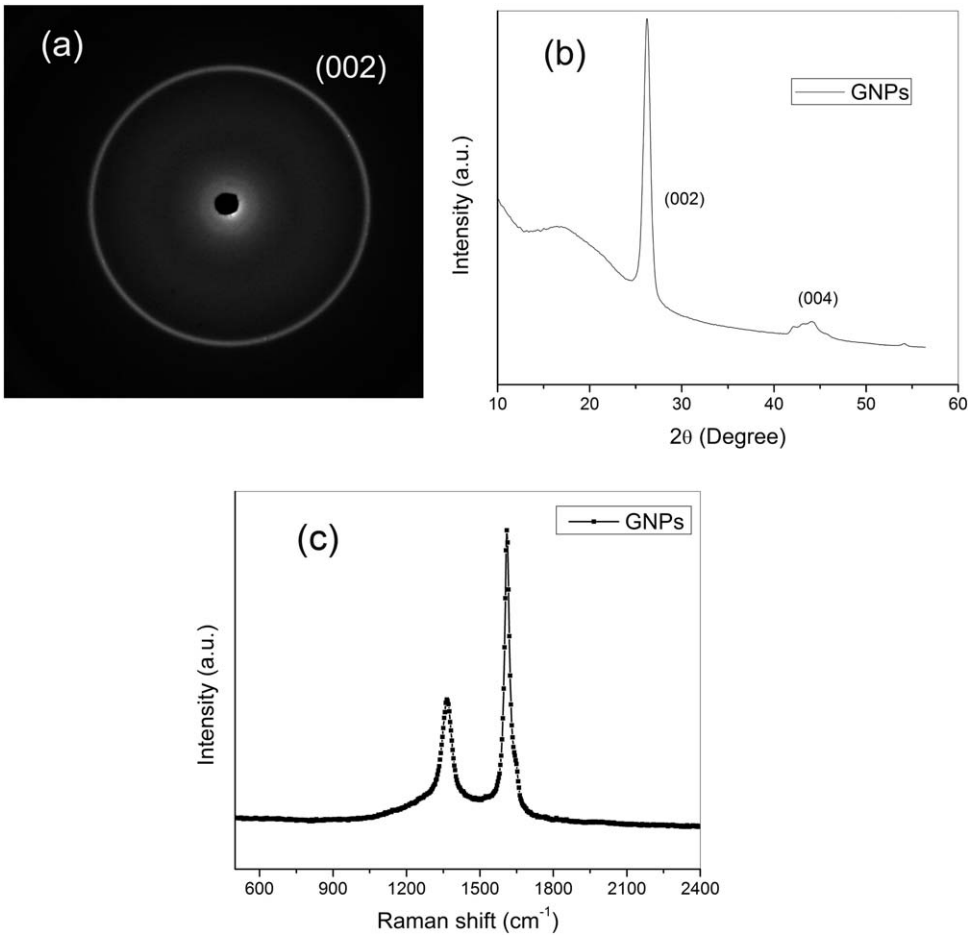

Figure 3. (a) Two-dimensional (2D) wide angle X-ray scattering (WAXS) of GNPs and (b) corresponding data conversion into 2θ values; (c) Raman spectrum of GNPs.

aids the mixing of the two dissimilar materials but also benefits the overall properties of the composites.[36–40] Fine dispersion of GNPs reduced the stress concentration sites, whereas the plasticizing effect operated in combination with interfacial adhesion between the filler and matrix to yield an increase in the toughness of the composites. Furthermore, even the Young's modulus of composites increased continuously with increasing GNPs contents, ultimate tensile strength of composite started to decrease above 2 wt %. It is due to the fact that the tensile strength is more sensitive to stress concentration sites, such as GNPs agglomerates and damage zones at high concentration of filler, than the Young's modulus. The tensile fracture surfaces of neat HDPE as well as 2 wt % GNPs/HDPE composite with titanate were observed to reveal the structural changes upon deformation. For the neat HDPE, it was clear that numerous HDPE particles deboned leaving large groove with plastic deformation

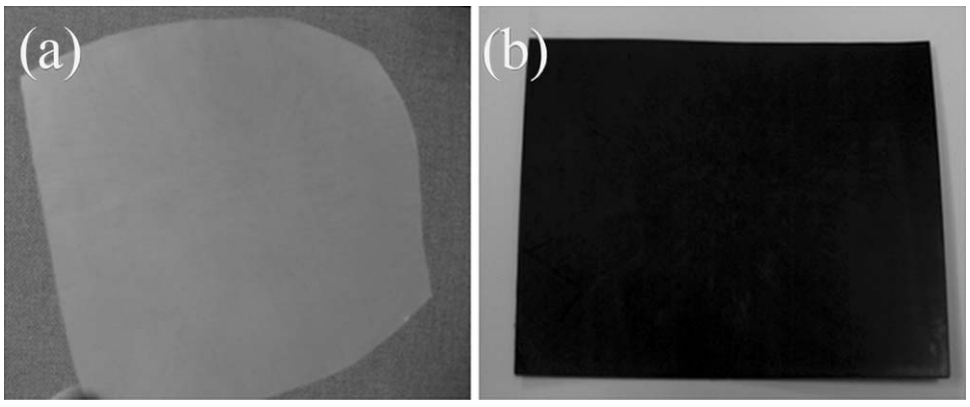

Figure 4. Photographs of (a) neat HDPE and (b) 2 wt % GNPs/HDPE composite thin film with titanate.

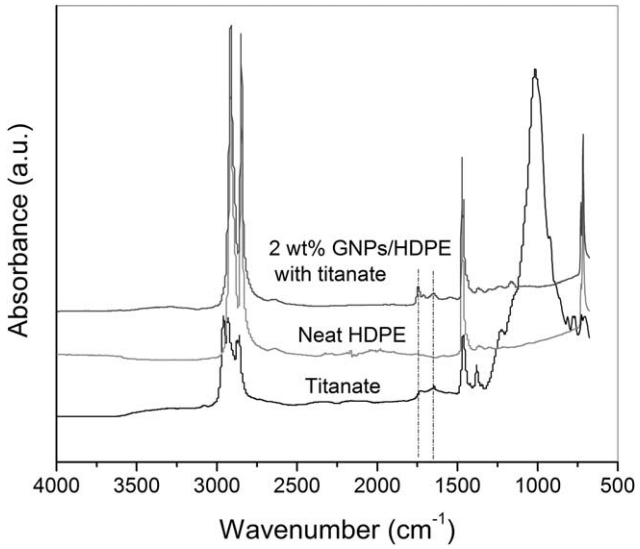

Figure 5. FTIR spectra of neoalkoxy titanate (LICA 12), neat HDPE, and 2 wt % GNPs/HDPE composite with titanate.

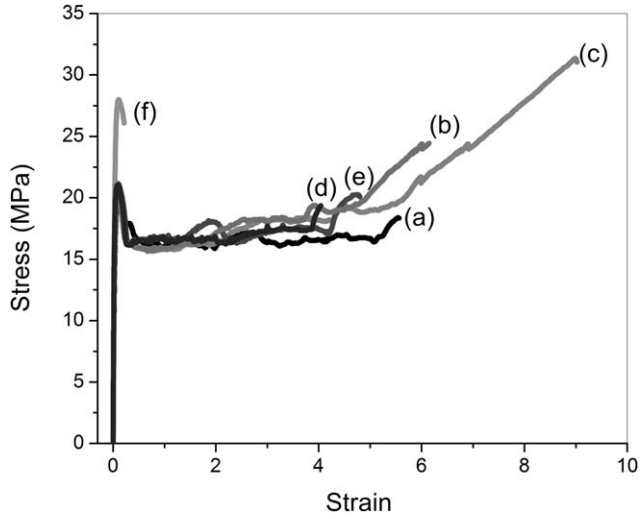

Figure 6. Tensile stress–strain curves of (a) neat HDPE, (b) 2 wt %, and (d) 5 wt % GNPs/HDPE composite without titanate. Tensile stress–strain curves of (c) 2 wt %, (e) 5 wt %, and (f) 10 wt % GNPs/HDPE composites with titanate.

(not shown). The SEM image of 2 wt % GNPs/HDPE composite with titanate in Figure 8 shows a typical ductile fracture with a considerable large plastic deformation. Here, the GNPs/HDPE composite in the fracture surfaces were deformed into numerous fibrils (Figure 8 insets). Thus, we concluded that the addition of titanate largely improved the elongation at break of the 2 wt % GNPs/HDPE composite than neat HDPE, which was responsible for the huge plastic deformation (fibrillation) of the GNPs/HDPE phase. However, at high concentration of GNPs in HDPE, probably the matrix defect due to the agglomeration of graphene dominated the mechanical performance of composite, as a result tensile strength as well as the elongation at break of composites were largely decreased [Figure 7(a,c)].

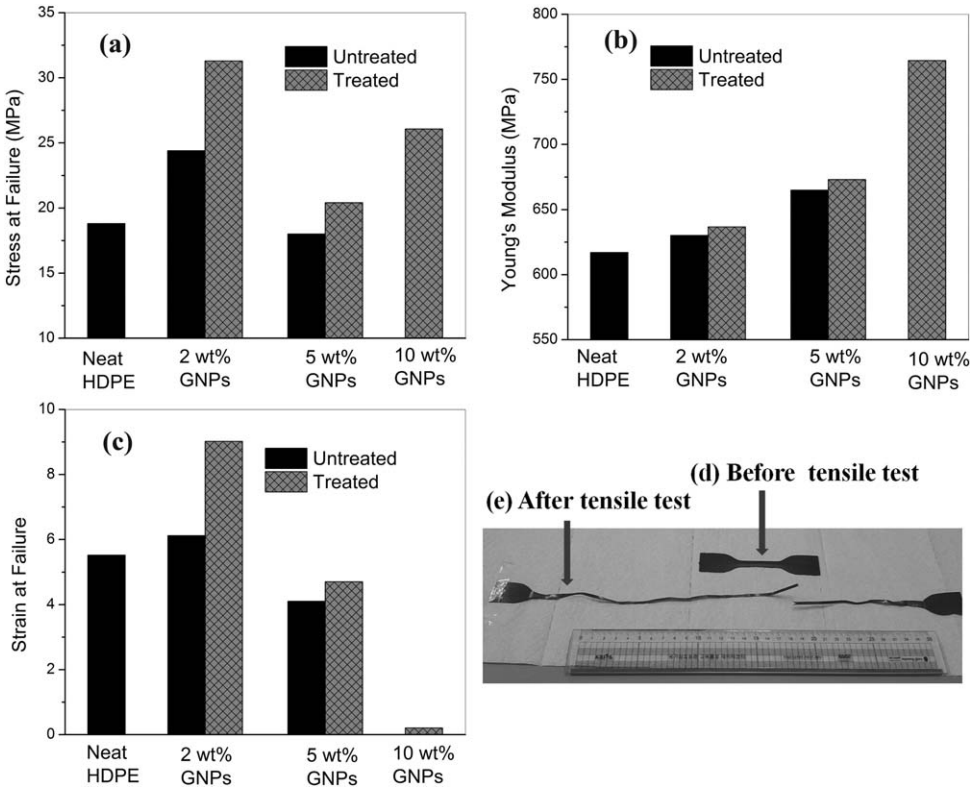

Figure 7. Change of (a) stress at failure, (b) Young's modulus, and (c) strain at failure as a function of GNPs content in GNPs/HDPE composites with and without titanate treatment. Optical image of 2 wt % GNPs/HDPE composite with titanate (d) before tensile test and (e) after tensile fracture.

Table I. Mechanical Properties of Neat HDPE and GNPs/HDPE Nanocomposites with and without Titanate

	E (MPa)	σ_b (MPa)	ϵ
Neat HDPE	617 ± 10	18.8 ± 0.8	5.52 ± 0.5
2 wt % GNPs/HDPE without titanate	630.2 ± 25	24.4 ± 1.5	6.12 ± 0.6
5 wt % GNPs/HDPE without titanate	665 ± 15	18 ± 1.3	4.1 ± 0.5
2 wt % GNPs/HDPE with titanate	636.7 ± 10	31.3 ± 1.5	9.02 ± 1.0
5 wt % GNPs/HDPE with titanate	673 ± 17	20.4 ± 1.2	4.7 ± 0.3
10 wt % GNPs/HDPE with titanate	764.52 ± 10	26.07 ± 0.5	0.21 ± 0.05

E, Young's modulus; σ_b, Elongation at break; and ϵ, Strain at failure.

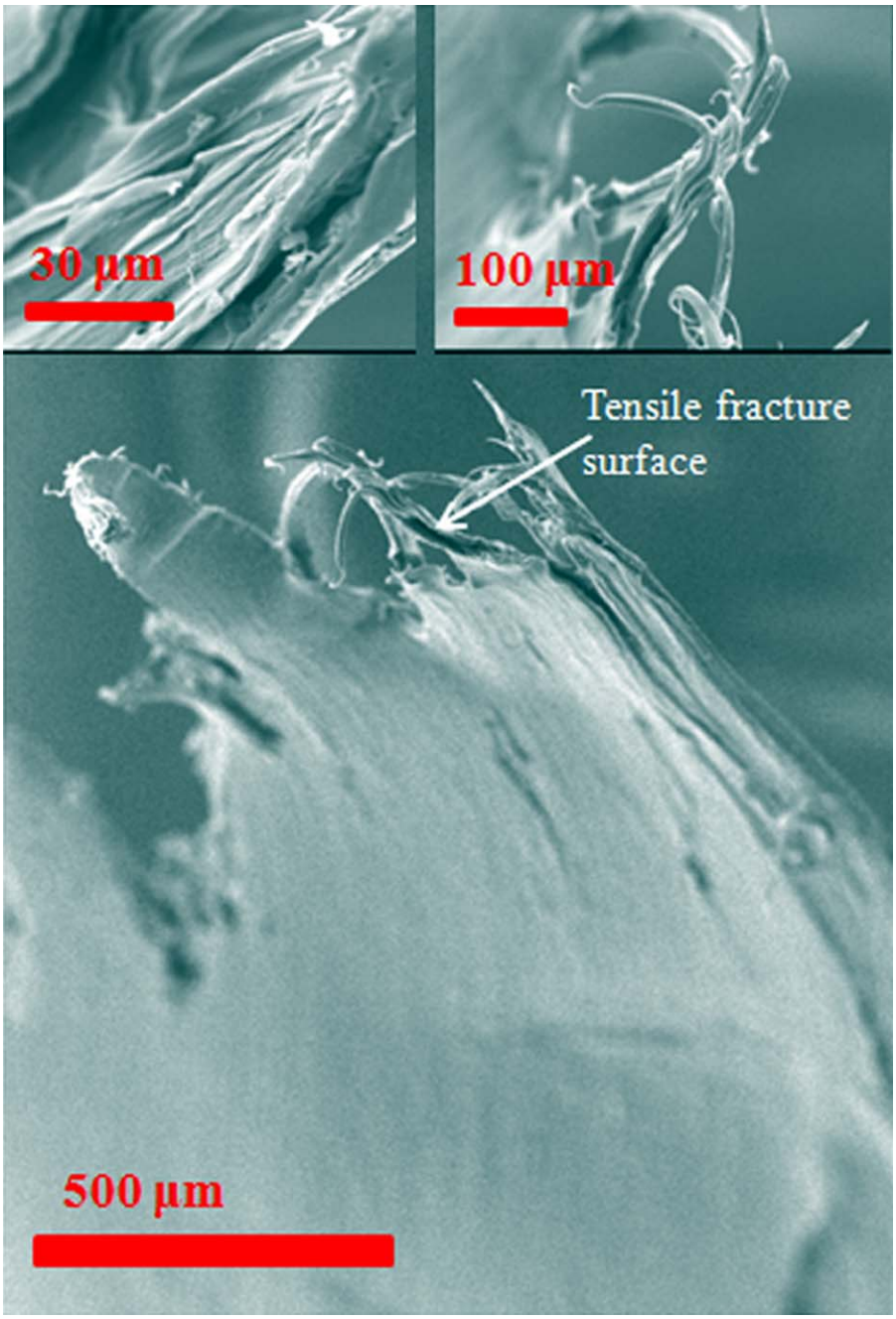

Figure 8. SEM images of the tensile fractured surfaces of the 2 wt % GNPs/HDPE composite with titanate. The insets are the corresponding fracture surface at high magnification. [Color figure can be viewed in the online issue, which is available at wileyonlinelibrary.com.]

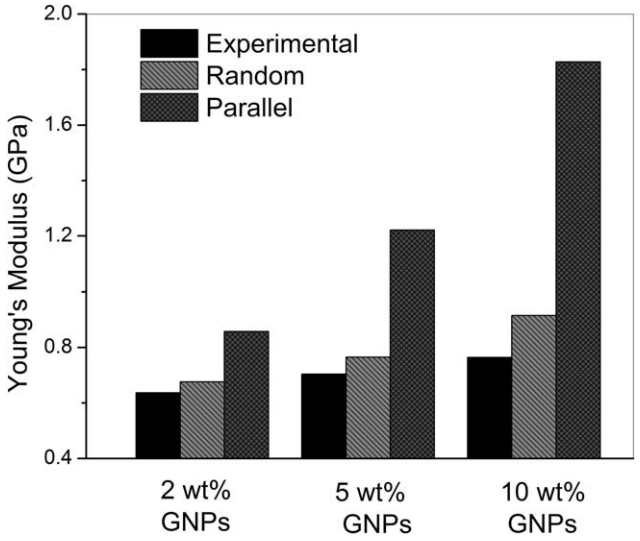

Figure 9. Comparison of experimental data of GNPs/HDPE composites and calculated data derived from Halpin–Tsai model under two extreme cases: the aligned and random dispersion of GNPs in the HDPE matrix.

The optical image of 2 wt % GNPs/HDPE composite with titanate (d) before tensile test and (e) after tensile fracture are shown in Figure 7. Here, we clearly observed that the original length of the specimen was largely increased after tensile test.

The Halpin–Tsai model has already employed to simulate the modulus of unidirectional or randomly distributed filler-based polymer composites.[19,35,41–43] In this model the tensile moduli of the matrix and filler as well as the aspect ratio and volume fraction of the fillers are substituted to predict the tensile modulus of composite materials. In this study, we observed small differences on the modulus of GNPs/HDPE composites with and without coupling agent. So, only the modulus of titanate treated GNPs based HDPE composites was used for the comparison with the theoretically predicted modulus. The Halpin–Tsai model eqs. (1) and (2) as shown below can be used to predict the composite tensile modulus in both the longitudinal direction and the transverse direction for unidirectional, discontinuous filler composites. Where E_L is the longitudinal HDPE composite tensile modulus, E_T is the transverse HDPE composite tensile modulus, E_{PE} is the tensile modulus of the neat HDPE, Φ is the volume fraction of filler, and ξ is the filler shape factor.[19,42] We assumed that GNPs used in this study act as an effective rectangular solid with a certain aspect ratio (a_g), length (L_f), and thickness (T_f). The statistical average values of L_f and T_f are 5.0 μm and 8.0 nm, respectively as measured by TEM. The parameters η_L and η_T are given in eqs. (3) and (4): where E_f is the tensile modulus of the filler. Graphene sheets have a tensile modulus of ~1 TPa in the plane of the sheet.[13] In GNPs, multiple graphene sheets stalked on each other. When the tensile loads are transferred to the GNPs from the HDPE, the van der Waals's force between graphene sheets is likely to fail before graphitic carbon–carbon bonding, leading to further exfoliation of the GNPs. Thus, the modulus of exfoliation in the graphite *c*-axis (through-the-plane) 36.5 GPa was used for the Halpin–Tsai model.[43] The Young's modulus of pure HDPE was obtained 0.62 GPa from our experimental data. Equation (6) was used for the random orientation of GNPs in composites. The theoretical predictions for randomly

$$E_L/E_{PE} = \frac{(1+\xi\eta_L\Phi)}{(1-\eta_L\Phi)} \quad (1)$$

$$E_L/E_{PE} = \frac{(1+2\eta_T\Phi)}{(1-\eta_T\Phi)} \quad (2)$$

$$\eta_L = \frac{(E_f/E_{PE})-1}{(E_f/E_{PE})+\xi} \quad (3)$$

$$\eta_T = \frac{(E_f/E_{PE})-1}{(E_f/E_{PE})+2} \quad (4)$$

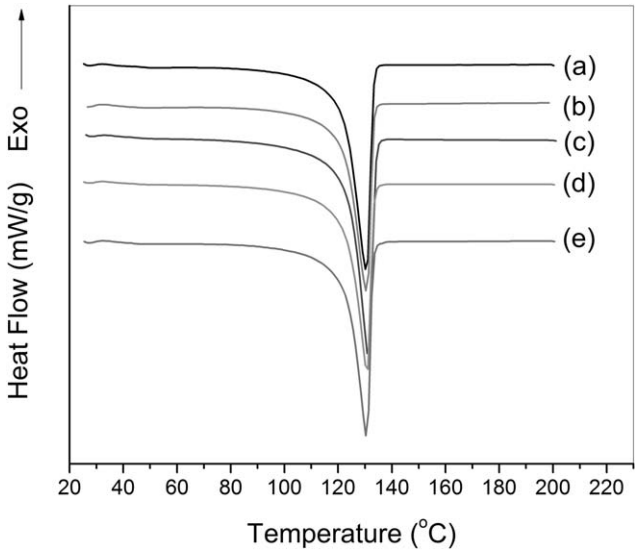

Figure 10. DSC thermograms of (a) neat HDPE and (b) 2 wt % GNPs/HDPE composite without titanate. DSC thermograms of (c) 2, (d) 5, and (e) 10 wt % GNPs/HDPE nanocomposites with titanate.

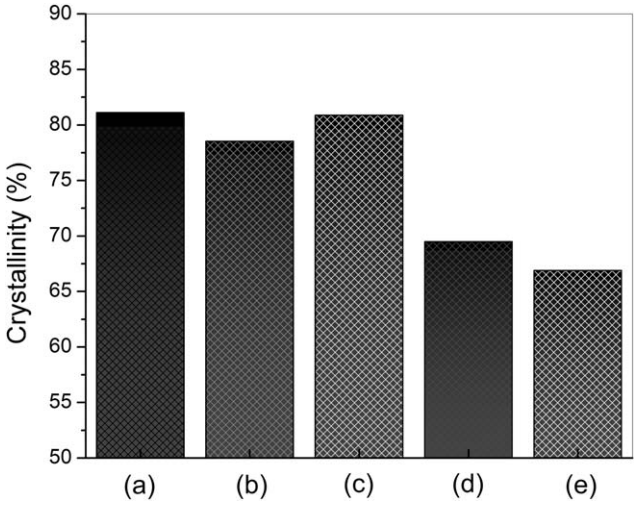

Figure 11. Crystallinity of (a) neat HDPE and (b) 2 wt % GNPs/HDPE composite without titanate. Crystallinity of titanate treated (c) 2 wt %, (d) 5 wt %, and (e) 10 wt % GNPs/HDPE nanocomposites.

Table II. T_m, T_c, ΔH_m, ΔH_c, and X_c of Neat HDPE and GNPs/HDPE Composites with and without Titanate from DSC

	T_m	T_c	ΔH_m (J/g)	ΔH_c (J/g)	Crystallinity (%)
Neat HDPE	130	118.6	162.3	144.0	81.1
2 wt % GNPs/HDPE without titanate	130	118.6	154.3	139.4	78.52
2 wt % GNPs/HDPE with titanate	131.2	118.4	162.1	143.5	80.86
5 wt % GNPs/HDPE with titanate	130.8	118.7	141.6	123.3	69.48
10 wt % GNPs/HDPE with titanate	130	118.6	141.1	118.7	66.89

$$\xi = 2a_g/3 = 2L_f/3T_f \quad (5)$$

$$E_C = (1/5)E_L + (4/5)E_T \quad \text{For randomly oriented filler} \quad (6)$$

dispersed filler throughout the matrix showed a close agreement with the experimental data obtained for the GNPs/HDPE composites (Figure 9). The value obtained for the theoretical modulus of unidirectional GNPs in HDPE showed a large deviation from the experimental data. This indicated that the GNPs are randomly distributed in the HDPE matrix. However, we believe that the plasticizing effect of titanate affected the modulus of HDPE composite as a result the modulus obtained from experimental data of 2 and 5 wt % composites are slightly lower than expected in our study. Furthermore, the theoretical aspect ratio of GNPs used for the calculations might be lower due to the aggregation as well as change of the platelet morphology (e.g., folding, roll-up, buckling) during processing of the 10 wt % HDPE composites as a result the value obtained from Halpin–Tsai model was larger than the experimental value.

DSC thermograms of (a) neat HDPE and (b) 2 wt % untreated GNPs/HDPE composite in Figure 10 confirm that the position of the melting peak of neat HDPE at 130.0°C was not changed even after 2 wt % GNPs loading. However, DSC thermograms of titanate treated (c) 2, (d) 5, and (e) 10 wt % GNPs/HDPE nanocomposites in Figure 10 show that the position of the melting peak of 2 wt % composite increased to 131.2°C and then started to decrease for 5 and 10 wt % composites towards the neat HDPE. Here, the increased value of the melting peak of titanate treated 2 wt % GNPs/HDPE composite indicates the positive interaction of GNPs with HDPE with titanate through proton coordination. Even the titanate showed plasticizing effect, good dispersion of GNPs in HDPE dominated the overall properties of composite as a result melting point of 2 wt % composite was increased. At high concentration of GNPs loading say 5 and 10 wt %, filler agglomeration might be influenced the overall properties. The % crystallinity of HDPE and GNPs/HDPE composite with and without titanate treatment is shown in Figure 11. The % crystallinity of HDPE (X_o) was calculated 81.1% based on the following equation:

$$X_o = \rho_c(\rho - \rho_a)/\rho(\rho_c - \rho_a) \quad (7)$$

where the density of the HDPE (ρ), 100% crystal HDPE (ρ_c), and completely amorphous HDPE (ρ_a) are 0.95, 0.985, and 0.825 g/cm^3, respectively.[44,45] It is obvious that the presence of GNPs is likely to influence the crystallization of HDPE as a result the mechanical performance of the resulting composites can also affect.

The % crystallinity of HDPE (X_c) in the nanocomposite was estimated based on the following equation:

$$X_c = X_D(\Delta H/\Delta H_o) \quad (8)$$

where the crystallization enthalpy per gram of pure HDPE (ΔH_o) and composites (ΔH_c) were obtained from the cooling run of DSC. The relative crystallinity of 2 wt % GNPs/HDPE composite with titanate (80.8%) was found almost equal to the neat HDPE (81.1%). But, further increasing the concentration of GNPs, the crystallinity of HDPE in 10 wt % composite was decreased to 66.89%. Generally, the crystalline domains of HDPE are formed smaller in the presence of nanomaterials and reduce the overall crystallinity with increasing the filler content.[45,46] Furthermore, in our study, we found small decreases in the crystallinity until 2 wt % loading of filler in HDPE. The decrease in crystallinity is also likely that imperfection of crystals in the presence of inhomogeneities that influences to decrease in crystallinity. Moreover, even the same concentration of GNPs loading (2 wt %) in HDPE, titanate treated composite showed higher crystallinity than without titanate due to the presence of better dispersed inhomogeneities inducing

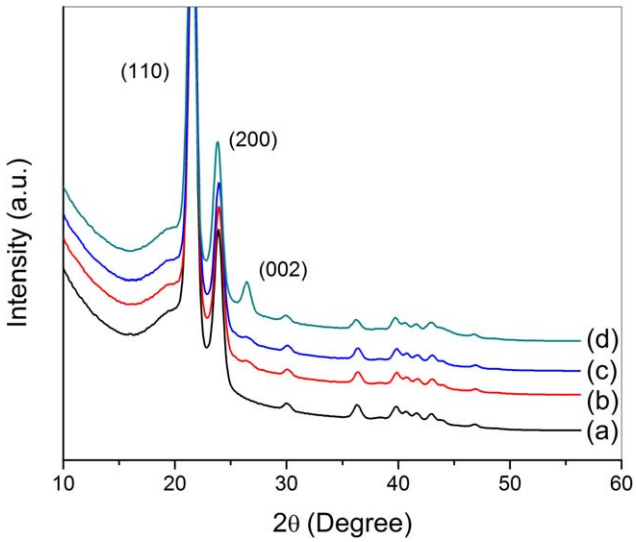

Figure 12. The wide angle X-ray scattering for (a) 0, (b) 2, (c) 5, and (d) 10 wt % GNPs/HDPE nanocomposites with titanate. [Color figure can be viewed in the online issue, which is available at wileyonlinelibrary.com.]

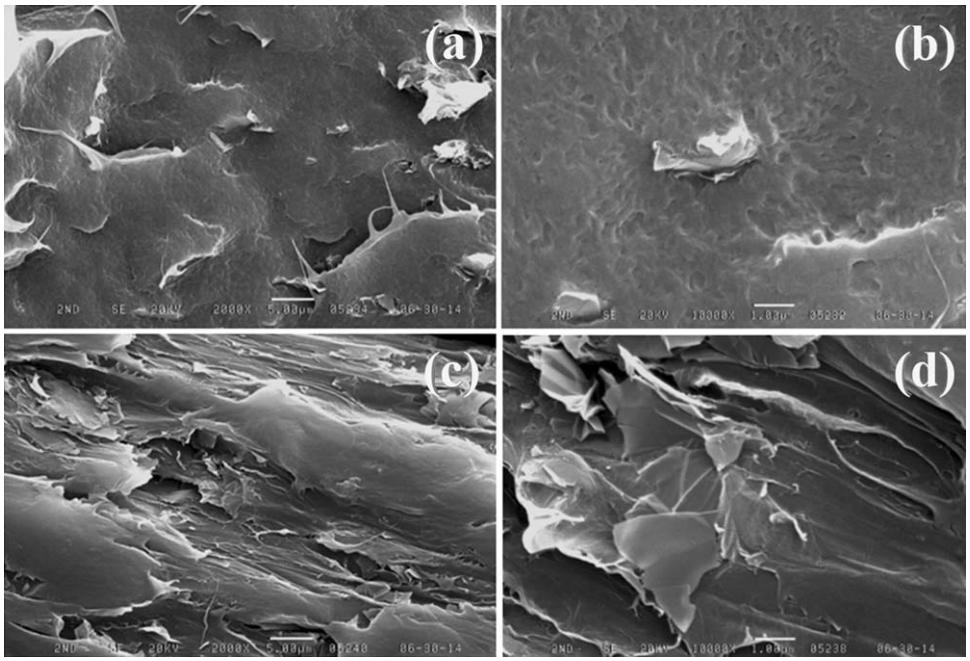

Figure 13. SEM micrographs of cryogenically fracture surface of (a and b) 2 wt % and (c and d) 5 wt % GNPs/HDPE composites with titanate. Scale bar is 5 μm for a and c and 1 μm for b and d.

crystallization.[45] At 5 and 10 wt % GNPs loading in HDPE, the mobility of HDPE chains in the formation of crystallites was hindered by GNPs, as a result the domains of crystalline phase are reduced in size. Table II shows the T_m, T_c, ΔH_m, ΔH_c, and % crystallinity of neat HDPE and GNPs/HDPE composites with and without titanate treatment. We found small changes on the ΔH_m, ΔH_c, and % crystallinity of HDPE by 2 wt % loading of GNPs with titanate. On the other hand, even 2 wt % GNPs loading without titanate and higher loading of GNPs (5 and 10 wt %) with titanate showed significantly decreased value of ΔH_m, ΔH_c, and % crystallinity due to the hindrance of the GNPs for the formation of crystal structure in the composites. At last, the stronger interaction was revealed in 2 wt % GNPs containing HDPE with titanate, which is in trustworthiness with the higher melting temperature.

Figure 12 shows the results of a wide angle X-ray scattering (WAXS) for neat HDPE and the composites obtained for this study. Neat HDPE possesses two major characteristic peaks for $2\theta = 21.44°$ and 23.75° from the (110) and (200) lattice plane of HDPE crystal, and the new peak of about $2\theta = 26.3°$ was found in 10 wt % GNPs/HDPE composites, corresponding to the (002) plane of GNPs. It is obvious that the peak intensity of the (002) lattice plane became stronger with increasing the GNPs content in composites. The morphology of the fracture surface of the GNPs/HDPE nanocomposites was specifically characterized by using SEM. Figure 13 presents SEM images of (a and b) 2 and (c and d) 5 wt % GNPs based HDPE composites with titanate at different magnification. Because of the strong interfacial interactions between the GNPs and HDPE through proton coordination with titanate, there was obvious structural perfection [Figure 11(a)]; this would be useful to improve the mechanical properties of the 2 wt % GNPs/HDPE composite. At high concentration of GNPs (say 5 wt %), agglomeration of GNPs at certain region as shown in Figure 11 (d) created matrix defect and that caused to decline the mechanical properties of composite.

CONCLUSIONS

In the current study, the thermal and mechanical properties of the titanate treated GNPs filled HDPE composites were investigated. We observed superior mechanical reinforcement effect in titanate treated 2 and 5 wt % GNPs/HDPE composites compared to untreated GNPs/HDPE composites. Here, the adsorbed titanate coupling agent on GNPs and HDPE through proton coordination improved the interfacial adhesion between the filler and matrix as a result composites with the coupling agent showed superior mechanical properties than untreated composites. The morphological analysis of the nanocomposite confirmed the fine dispersion of 2 wt % GNPs in HDPE with titanate. The tensile test of 2 wt % GNPs/HDPE nanocomposites with titanate showed 66.5% improvement of ultimate tensile strength with enormously high value of elongation at break. The strong strain hardening effect was responsible to improve the ultimate tensile strength of 2 wt % GNP/HDPE composite. The plasticizing effect of titanate was suppressed with the incorporation of higher concentration of GNPs as a result 10 wt % GNPs/HDPE composites showed 24% improvement of Young's modulus. Finally, the large improvement on the ultimate tensile strength and the toughness of the 2 wt % composites could be attributed to the improved dispersion as well as orientation of GNPs towards strain direction.

ACKNOWLEDGMENTS

This work was supported by the Nuclear Power Core Technology Development Program of the Korea Institute of Energy Technology Evaluation and Planning (KETEP) granted financial resource from the Ministry of Trade, Industry & Energy, Republic of Korea (Project No. 20131510200400).

REFERENCES

1. Chung, T. C. *Prog. Polym. Sci.* **2002**, *27*, 39.
2. Zhao, Y.; Wang, L.; Xiao, A.; Yu, H. *Prog. Polym. Sci.* **2010**, *35*, 1195.
3. Godoy Lopez, R.; D'Agosto, F.; Boisson, C. *Prog. Polym. Sci.* **2007**, *32*, 419.
4. Li, Y.-C.; Chen, G.-H. *Polym. Eng. Sci.* **2007**, *47*, 882.
5. Chaudhry, A. U.; Mittal, V. *Polym. Eng. Sci.* **2013**, *53*, 78.
6. Pollanen, M.; Pirinen, S.; Suvanto, M.; Pakkanen, T. T. *Compos. Sci. Technol.* **2011**, *71*, 1353.
7. Wang, L.; Hong, J.; Chen, G. *Polym. Eng. Sci.* **2010**, *50*, 2176.
8. Seo, H. M.; Park, J. H.; Dao, T. D.; Jeong, H. M. *J. Nanomater.* **2013**, *2013*, 8.
9. Chen, G.; Chen, X.; Wang, H.; Wu, D. *J. Appl. Polym. Sci.* **2007**, *103*, 3470.
10. Mittal, V.; Luckachan, G. E.; Matsko, N. B. *Macromol. Chem. Phys.* **2014**, *215*, 255.
11. Pang, H.; Yan, D.-X.; Bao, Y.; Chen, J.-B.; Chenb, C.; Li, Z.-M. *J. Mater. Chem.* **2012**, *22*, 23568.
12. Achaby, M. E.; Qaiss, A. *Mater. Des.* **2013**, *44*, 81.
13. Geim, A. K.; Novoselov, K. S. *Nat Mater.* **2007**, *6*, 183.
14. Truong, Q.-T.; Pokharel, P.; Song, G. S.; Lee, D. S. *J. Nanosci. Nanotechnol.* **2012**, *12*, 4305.
15. Pokharel, P.; Lee, S. H.; Lee, D. S. *J. Nanosci. Nanotech.* **2015**, *15*, 211.
16. Pokharel, P.; Choi, S.; Lee, D. S. *Compos. Part A* **2015**, *69*, 168.
17. Pokharel, P.; Truong, Q.-T.; Lee, D. S. *Compos. Part B* **2014**, *64*, 187.
18. Pant, H. R.; Pant, B.; Pokharel, P.; Kim, H. J.; Tijing, L. D.; Park, C. H.; Lee, D. S.; Kim, H. Y.; Kim, C. S. *J. Member. Sci.* **2013**, *429*, 225.
19. Pokharel, P.; Lee, D. S. *Chem. Eng. J.* **2014**, *253*, 356.
20. Micusik, M.; Omastova, M.; Krupa, I.; Prokes, J.; Pissis, P.; Logakis, E.; Pandis, C.; Potschke, P.; Pionteck, J. *J. Appl. Polym. Sci.* **2009**, *113*, 2536.
21. Pokharel, P.; Lee, D. S. *J. Nanosci. Nanotechnol.* **2014**, *14*, 5718.
22. Pollanen, M.; Pirinen, S.; Suvanto, M.; Pakkanen, T. T. *Compos. Sci. Technol.* **2011**, *71*, 1353.
23. Waha, C. A.; Choongb, L. Y.; Neon, G. S. *Eur. Polym. J.* **2000**, *36*, 789.
24. lhssain, M.; Nakahira, A.; Nishijima, S.; Niihara, K. *Mater. Lett.* **1996**, *26*, 299.
25. Gonzalez, J.; Albano, C.; Ichazo, M.; Diaz, B. *Eur. Polym. J.* **2002**, *38*, 2465.
26. Choi, S.-S.; Kim, J-. C.; Ko, J.-E.; Cho, Y. S.; Shin, W. G. *J. Ind. Eng. Chem.* **2007**, *13*, 1017.
27. Wang, Y.; Wang, J.-J. *Polym. Eng . Sci.* **1999**, *39*, 190.
28. Gutowski, W. S.; Wu, D. Y.; Li, S. US Pat. 005879757A (**1999**).
29. Molitor, P.; Barron, V.; Young, T. *Int. J. Adhes. Adhes.* **2001**, *21*, 129.
30. Alkadasi, N. A. N.; Sarwade, B. D.; Hundiwale, D. G.; Kapadi, U. R. *J. Appl. Polym. Sci.* **2004**, *93*, 1293.
31. Monte, S. J. Reference Manual-Titanate, Zirconate and Aluminate Coupling Agents; American Chemical Society: Washington, DC, **1995**.
32. Li, J.; Yang, Z.; Qiu, H.; Dai, Y.; Zheng, Q.; Zheng, G.-P.; Yang, J. *J. Mater. Chem. A* **2013**, *1*, 11451.
33. Leong, Y. W.; Abu Bakar, M. B.; Mohd Ishak, Z. A.; Ariffin, A. *J. Appl. Polym. Sci.* **2005**, *98*, 413.
34. Monte, S. J.; Sugerman, G. *Polym. Eng. Sci.* **1984**, *24*, 1369.
35. Kalaitzidou, K.; Fukushima, H.; Miyagawa, H.; Drzal, L. T. *Polym. Eng. Sci.* **2007**, *47*, 1796.
36. Hu, H.; Zhang, G.; Xiao, L.; Wang, H.; Zhao, Q. Z. Z. *Carbon* **2012**, *50*, 4596.
37. Jiang, X.; Drzal, L. T. *Polym. Compos.* **2012**, *33*, 636.
38. Wang, Q.; Gao, J.; Wang, R.; Hua, Z. *Polym. Compos.* **2001**, *22*, 97.
39. Deb, S.; Wang, M.; Tanner, K. E.; Bonfield, W. *J. Mater. Sci.: Mater. Med.* **1996**, *7*, 191.
40. Chen, J.; Maekawa, Y.; Yoshida, M.; Tsubokawa, N. *Polym. J.* **2002**, *34*, 30.
41. Liang, J.; Huang, Y.; Zhang, L.; Wang, Y.; Ma, Y.; Guo, T.; Chen, Y. *Adv. Funct. Mater.* **2009**, *19*, 1.
42. Rafiee, M. A.; Rafiee, J.; Wang, Z.; Song, H.; Yu, Z. Z.; Koratkar, N. *ACS Nano* **2009**, *3*, 3884.
43. King, J. A.; Klimek, D. R.; Miskioglu, I.; Odegard, G. M. *J. Appl. Polym. Sci.* **2013**, *128*, 4217.
44. Peacock, A. J. Handbook of Polyethylene, Structure, Properties, and Applications. Marcel Dekker: New York, **2000**.
45. Zheng, W.; Lu, X.; Wong, S.-C. *J. Appl. Polym. Sci.* **2004**, *91*, 2781.
46. Mirabella, F. M.; Bafna, A. *J. Polym. Sci.: Part B: Polym. Phys.* **2002**, *40*, 1637.